

# Pixel-by-pixel local dimming for high-dynamic-range liquid crystal displays

HAIWEI CHEN,<sup>1</sup> RUIDONG ZHU,<sup>1</sup> MING-CHUN LI,<sup>2</sup> SEOK-LYUL LEE,<sup>2</sup> AND SHIN-TSON WU<sup>1,\*</sup>

<sup>1</sup>College of Optics and Photonics, University of Central Florida, Orlando, Florida 32816, USA

<sup>2</sup>AU Optronics Corp., Hsinchu Science Park, Hsinchu 300, Taiwan

\*swu@ucf.edu

**Abstract:** We propose a high dynamic range (HDR) liquid crystal display (LCD) with pixel-level local dimming. The device structure consists of a pixelated LCD dimming panel to control the backlight intensity entering the master LCD panel. According to our analysis and test cell experiment, this dual-panel display system possesses exceedingly high contrast ratio ( $> 1,000,000:1$ ) and high bit-depth ( $> 14$  bits) at merely 5 volts. Meanwhile, to mitigate the Moiré effect induced by the cascaded thin-film transistor (TFT) backplanes, we separate the two LCD panels with a polarization-dependent scattering film. The pros and cons of this HDR display are discussed.

© 2017 Optical Society of America

**OCIS codes:** (230.3720) Liquid-crystal devices; (120.2040) Displays; (310.6845) Thin film devices and applications.

## References and links

1. H. Seetzen, W. Heidrich, W. Stuerzlinger, G. Ward, L. Whitehead, M. Trentacoste, A. Ghosh, and A. Vorozcovs, "High dynamic range display systems," *ACM Trans. Graph.* **23**(3), 760–768 (2004).
2. J. U. Kwon, S. Bang, D. Kang, and J. J. Yoo, "The required attribute of displays for high dynamic range," *SID Symp. Dig. Tech. Papers* **47**(1), 884–887 (2016).
3. S. Daly, T. Kunkel, X. Sun, S. Farrell, and P. Crum, "Viewer preferences for shadow, diffuse, specular, and emissive luminance limits of high dynamic range displays," *SID Symp. Dig. Tech. Papers* **44**(1), 563–566 (2013).
4. C. H. Oh, H. J. Shin, W. J. Nam, B. C. Ahn, S. Y. Cha, and S. D. Yeo, S.D., "Technological progress and commercialization of OLED TV," *SID Symp. Dig. Tech. Papers* **44**(1), 239–242 (2013).
5. H. Chen, T. H. Ha, J. H. Sung, H. R. Kim, and B. H. Han, "Evaluation of LCD local-dimming-backlight system," *J. Soc. Inf. Disp.* **18**(1), 57–65 (2010).
6. F. C. Lin, Y. P. Huang, L. Y. Liao, C. Y. Liao, H. P. D. Shieh, T. M. Wang, and S. C. Yeh, "Dynamic backlight gamma on high dynamic range LCD TVs," *J. Disp. Technol.* **4**(2), 139–146 (2008).
7. K. Nakajima, H. Tsuchi, Y. Hori, T. Nose, H. Furihata, K. Umeda, and J. Ishii, "A 12-bit LCD source driver IC with point-to-point link interface," *SID Symp. Dig. Tech. Papers* **38**(1), 1633–1635 (2007).
8. K. J. Kwon, M. B. Kim, C. Heo, S. G. Kim, J. S. Baek, and Y. H. Kim, "Wide color gamut and high dynamic range displays using RGBW LCDs," *Displays* **40**, 9–16 (2015).
9. D. Lanman, M. Hirsch, Y. Kim, and R. Raskar, "Content-adaptive parallax barriers: optimizing dual-layer 3D displays using low-rank light field factorization," *ACM Trans. Graph.* **29**(6), 163 (2010).
10. Y. Kitagawa, H. Ikeno, S. Uehara, and T. Yatsushiro, "Dual panel liquid crystal display device," U.S. Patent 7,916,223 (March 29, 2011).
11. D. Lanman, G. Wetzstein, M. Hirsch, W. Heidrich, and R. Raskar, "Polarization fields: dynamic light field display using multi-layer LCDs," *ACM Trans. Graph.* **30**(6), 186 (2011).
12. F. C. Huang, K. Chen, and G. Wetzstein, "The light field stereoscope: immersive computer graphics via factored near-eye light field displays with focus cues," *ACM Trans. Graph.* **34**(4), 60 (2015).
13. M. Schadt and W. Helfrich, "Voltage-dependent optical activity of a twisted nematic liquid crystal," *Appl. Phys. Lett.* **18**(4), 127–128 (1971).
14. A. Takeda, S. Kataoka, T. Sasaki, H. Chida, H. Tsuda, K. Ohmuro, T. Sasabayashi, Y. Koike, and K. Okamoto, "A super-high image quality multi-domain vertical alignment LCD by new rubbing-less technology," *SID Symp. Dig. Tech. Papers* **29**(1), 1077–1080 (1998).
15. S. H. Lee, S. L. Lee, and H. Y. Kim, "Electro-optic characteristics and switching principle of a nematic liquid crystal cell controlled by fringe-field switching," *Appl. Phys. Lett.* **73**(20), 2881–2883 (1998).
16. H. Chen, F. Peng, Z. Luo, D. Xu, S. T. Wu, M. C. Li, S. L. Lee, and W. C. Tsai, "High performance liquid crystal displays with a low dielectric constant material," *Opt. Mater. Express* **4**(11), 2262–2273 (2014).
17. H. Chen, R. Zhu, J. Zhu, and S. T. Wu, "A simple method to measure the twist elastic constant of a nematic liquid crystal," *Liq. Cryst.* **42**(12), 1738–1742 (2015).

18. A. Chao, K. T. Huang, C. W. Tsai, Y. W. Hung, H. F. Cheng, W. Yeh, C. H. Yu, and H. H. Wu, "The fastest response TN-type TFT LCD of the world likes OCB level," *SID Symp. Dig. Tech. Papers* **38**(1), 603–606 (2007).
19. H. Chen, Z. Luo, D. Xu, F. Peng, S. T. Wu, M. C. Li, S. L. Lee, and W. C. Tsai, "A fast-response A-film-enhanced fringe field switching liquid crystal display," *Liq. Cryst.* **42**(4), 537–542 (2015).
20. H. Chen, M. Hu, F. Peng, J. Li, Z. An, and S. T. Wu, "Ultra-low viscosity liquid crystals," *Opt. Mater. Express* **5**(3), 655–660 (2015).
21. F. Peng, H. Chen, F. Gou, Y. H. Lee, M. Wand, M. C. Li, S. L. Lee, and S. T. Wu, "Analytical equation for the motion picture response time of display devices," *J. Appl. Phys.* **121**(2), 023108 (2017).
22. H. Chen, F. Peng, F. Gou, Y. H. Lee, M. Wand, and S. T. Wu, "Nematic LCD with motion picture response time comparable to organic LEDs," *Optica* **3**(9), 1033–1034 (2016).
23. E. Jang, S. Jun, H. Jang, J. Lim, B. Kim, and Y. Kim, "White-light-emitting diodes with quantum dot color converters for display backlights," *Adv. Mater.* **22**(28), 3076–3080 (2010).
24. R. Zhu, Z. Luo, H. Chen, Y. Dong, and S. T. Wu, "Realizing Rec. 2020 color gamut with quantum dot displays," *Opt. Express* **23**(18), 23680–23693 (2015).
25. H. Chen, J. He, and S. T. Wu, "Recent Advances on Quantum-Dot-Enhanced Liquid Crystal Displays," *IEEE J. Sel. Top. Quantum Electron.* In press (2017).
26. G. Guarnieri, L. Albani, and G. Ramponi, "Minimum-error splitting algorithm for a dual layer LCD display—Part I: Background and theory," *J. Disp. Technol.* **4**(4), 383–390 (2008).
27. G. Guarnieri, L. Albani, and G. Ramponi, "Minimum-error splitting algorithm for a dual layer LCD display—Part II: Implementation and results," *J. Disp. Technol.* **4**(4), 391–397 (2008).
28. A. Moheghi, H. Nemati, and D. K. Yang, "Polarizing light waveguide plate from polymer stabilized liquid crystals," *Opt. Mater. Express* **5**(5), 1217–1223 (2015).
29. A. Moheghi, G. Qin, and D. K. Yang, "Stable polarizing light waveguide plate for edgelit liquid crystal displays," *Opt. Mater. Express* **6**(2), 429–435 (2016).

## 1. Introduction

High dynamic range (HDR) is a critical technology for next-generation displays, as it enables the viewer to see supreme image qualities, including higher contrast ratio (CR), darker black state, more gray levels and more vivid colors [1]. To achieve HDR, three basic requirements should be fulfilled: (1) high CR, (2) excellent black state and high peak brightness, and (3) precise control on how and where all these different bright and dark shades be applied to the displayed images [2]. To enlarge CR, both peak brightness and dark state should be improved [3]. For example, the luminance of bright state should be  $> 1000$  nits, while dark state should be  $< 0.01$  nits. In other words, the effective CR is over 100,000:1. For an organic light-emitting diode (OLED) display, it is fairly easy to get true black state, but to obtain a brightness over 1000 nits would lead to compromised lifetime [4]. On the contrary, it is relatively easy to boost an LCD's peak brightness to 1000 nits, but to lower the dark state to  $< 0.01$  nits is challenging. A typical CR of a multi-domain vertical alignment (MVA) LCD is  $\sim 5000:1$ , which is about 20x lower than what HDR demands. To improve dark state, local dimming technique has been commonly practiced [5, 6].

If a LCD's CR can be improved by 20x, then more grayscales can be displayed. For a standard dynamic range (SDR) display, 8-bit signal depth is commonly used. However for HDR, at least 10-bit depth is required [2]. The increased bit depth introduces splendid image quality, but may also bring heavier burden to the driving schemes. For thin-film-transistor (TFT) LCDs, the minimal voltage interval between two adjacent gray levels is about 8 mV. Then to achieve 10-bit depth (i.e. 1024 gray levels), the required on-state voltage is 8.19 V. If the signal depth is increased to 12 bits or even 14 bits, then the corresponding on-state voltage is 32.77 V and 131 V, respectively. Such a high operation voltage is beyond what the present TFT can provide. There is an urgent need to increase the bit depth while keeping a low operation voltage [7]. The final requirement of HDR is pixel-level local dimming. For OLED, each pixel is controlled from black state to full bright state easily. But for LCD, the presently employed local dimming is to divide LED backlight into hundreds of segments; it is far from the pixel-level local dimming. With some algorithm optimization, dimming accuracy can be improved [8], but the cost and complexity would also increase. Therefore, how to get HDR LCD with pixel-by-pixel local dimming remains a big challenge.

In this paper, we demonstrate a HDR LCD with two cascaded panels. In fact, dual-layer or even multi-layer LCD has already been widely used in 3D display, volumetric display and light field display [9–12], but few reports are focused on their electro-optical properties. Here, we perform systematic investigations on the dual-panel HDR LCD system, with special emphases on contrast ratio, gray level, operation voltage, response time, viewing angle, and Moiré effect. Our analysis and test cell experimental results indicate that we are able to achieve CR >1,000,000:1 (limited by the noises of our photodiode detector), high bit depth (>14 bits), low operation voltage (~5V), and pixel-level local dimming. To eliminate the Moiré patterns induced by the cascaded TFT backplanes, we introduced a polarization dependent scattering film (PDSF). Potential concerns for the dual-layer system are discussed, such as increased panel thickness, weight, cost, misalignment effect, and reduced optical efficiency. We believe such a HDR LCD would find widespread applications for medical imaging, art designing, movies, and vehicular displays.

## 2. Design of cascaded LCD panels

Figure 1 shows the proposed device configuration, consisting of a master display panel (LCD #2) and a pixelated dimming panel (LCD #1). In principle, any two LC modes can be paired up [13–15], e.g. VA and 90° TN (twisted nematic), VA and FFS (fringe-field switching), FFS and TN, two TNs, or two FFSs, just to name a few. However, considering the viewing angle, color shift, and cost, we choose FFS as master display and black-and-white TN (same dimension but without color filters) as local dimmer. TN is a normally-white broadband half-wave plate [14]; that means, at  $V = 0$  the incident white light passes through the TN panel and reaches the master display with high efficiency. If the local dimming is on demand, we can apply different voltages (through TFTs) to those chosen pixels to control their transmittance. While for the FFS panel [15], it shows excellent image quality, including wide viewing angle, unnoticeable color shift, weak gamma shift, and pressure resistance for touch panels. Therefore, we put it in the viewer side. Later, we will use the FFS/TN test cell results to illustrate the operation principles. Let us assume the contrast ratio of the two LCD panels is  $CR_1$  and  $CR_2$ , respectively. Then for the cascaded display system, the effective contrast ratio should be  $CR_1 * CR_2$  [1]. A typical CR for FFS LCD is ~2000:1 and TN is ~800:1, thus ideally the intrinsic CR of dual panels should be 1,600,000:1. Another advantage of this design is pixel-level local dimming, similar to OLED, if two panels are aligned well. Of course, there are some drawbacks, like decreased efficiency, increased cost, and misalignment issue. We will discuss these factors in detail later.

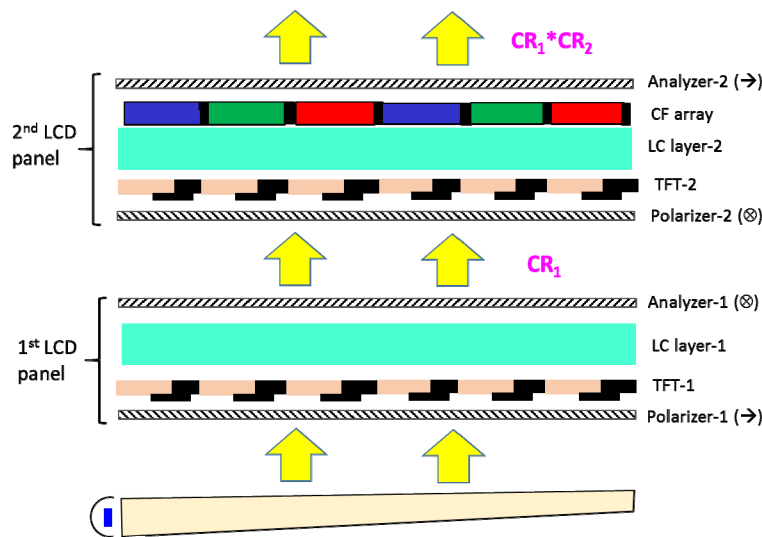


Fig. 1. Schematic diagram of the proposed structure with dual LCD panels.

### 3. Experiment and simulation results

Here, we perform experiment and simulation using the FFS and TN combination as an example. Unless otherwise mentioned, all the experiments were carried out at room temperature.

#### 3.1 VT curves

In experiment, we prepared one TN test cell with cell gap  $d = 5 \mu\text{m}$  and one FFS test cell with cell gap  $d = 3.5 \mu\text{m}$ . The employed LC (MLC-6686, Merck) material parameters are: birefringence  $\Delta n = 0.0983$  @  $\lambda = 550 \text{ nm}$  and dielectric anisotropy  $\Delta\epsilon = 10.0$  [16]. A He-Ne laser with  $\lambda = 633 \text{ nm}$  was used as probe beam. During measurement, the LC cell was driven by a square-wave voltage at 1 kHz frequency. The applied voltage was controlled by a LabVIEW (National Instruments) system. The measured voltage-dependent transmittance (VT) curves for both cells are plotted in Fig. 2. As expected, the TN test cell shows  $\sim 100\%$  transmittance (normalized to two parallel polarizers) and the dark state occurs at  $V = 3 V_{\text{rms}}$ . It is a perfect candidate for backlight local dimming. While for the FFS test cell (electrode width =  $4 \mu\text{m}$ , and electrode gap =  $3 \mu\text{m}$ ), its peak transmittance at  $\lambda = 633 \text{ nm}$  is 73.6% and  $V_{\text{on}} = 4.2 \text{ V}$ . If a low  $\Delta\epsilon$  LC mixture is employed, higher transmittance can be obtained, but at a slightly higher voltage [16].

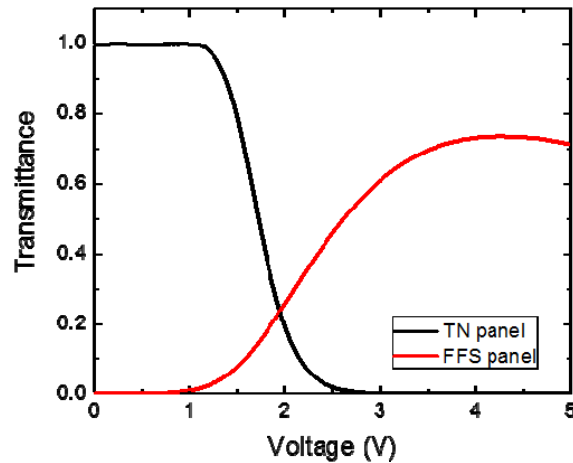


Fig. 2. Measured VT curves for TN and FFS test cells. LC: MLC-6686 with  $\Delta\epsilon = 10$ . FFS cell:  $d = 3.5 \mu\text{m}$ , electrode width  $\omega = 4 \mu\text{m}$ , and electrode gap  $l = 3 \mu\text{m}$ .  $\lambda = 633 \text{ nm}$ .

### 3.2 Contrast ratio

Next, we measured the contrast ratio of these two test cells. Results are  $\text{CR}_{\text{FFS}} = 4625:1$  and  $\text{CR}_{\text{TN}} = 2172:1$ . When we placed these two cells in sequence (TN is closer to the light source), in principle the CR should reach  $9,263,580:1$  ( $\text{CR}_{\text{FFS}} \cdot \text{CR}_{\text{TN}}$ ), but in experiment we only obtained  $\text{CR} = 1,102,564:1$  when the TN cell was driven at  $3 V_{\text{rms}}$ . This result is 8.4x smaller than the theoretical value, but still much higher than the required  $100,000:1$  for HDR displays. The reduced CR could be limited by the sensitivity of the photodiode detector we employed. Please note that, here linear polarizers with a high extinction ratio ( $\sim 18,000:1$ ) were adopted, and the measurement was performed using a He-Ne laser ( $\lambda = 633 \text{ nm}$ ). As a result, the obtained CR would be higher than the traditional value using a white backlight.

### 3.3 Response time

Figures 3(a) and 3(b) show the measured response time for the FFS cell and TN cell, respectively. Due to the small twist elastic constant [17], FFS cell exhibits a slower response time [rise time: 24.5 ms, decay time: 21.6 ms]; while for TN cell, the measured response time is relatively fast [decay time: 4.4 ms, rise time: 9.7 ms]. Then we combine FFS cell and TN cell together, and investigate the response time of dual-panel system. Results are plotted in Fig. 3(c), where rise time is 19.0 ms, and decay time is 6.4 ms. Interestingly, both rise time and decay time are improved as compared to single FFS cell, especially for decay time (21.6 ms vs. 6.4 ms). It means TN panel helps to accelerate the total transition process effectively. If we use a thinner cell gap with higher  $\Delta n$  yet low viscosity LC, an even faster response time ( $< 2 \text{ ms}$ ) can be achieved [18–20]. That way, its motion picture response time would be comparable to that of an OLED display, leading to much suppressed image blurs [21, 22].

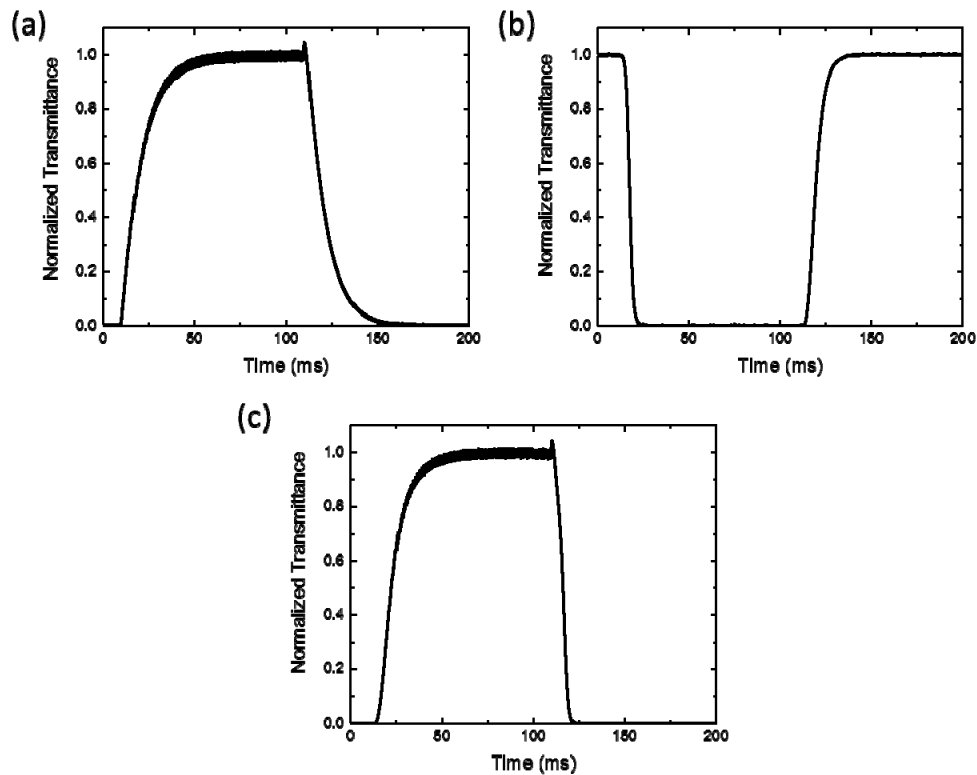


Fig. 3. Measured response time for (a) single FFS cell, (b) single TN cell, and (c) combined FFS + TN cell.

### 3.4 Signal depth

In real applications, two TFT LCD panels are driven independently. That is, TN panel provides pixel-by-pixel dimming, which controls the amount of backlight entering the FFS cell. For example, Fig. 4 shows the transmittance of the FFS/TN combined cell when the TN cell was operated at four different gray levels (25%, 50%, 75% and 100%), while the FFS cell is working normally from dark to bright states continuously.

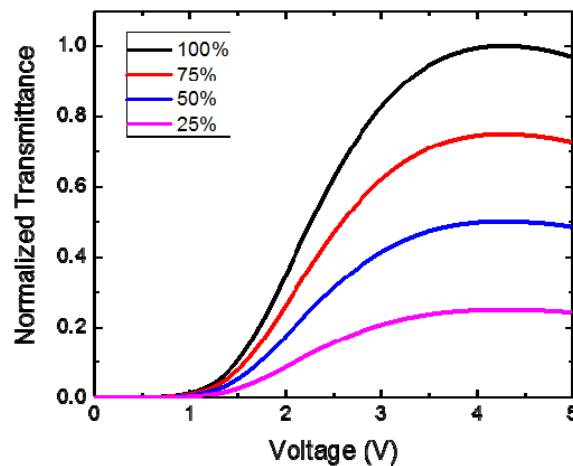


Fig. 4. Measured VT curves of FFS/TN when the TN cell is at 4 specified transmittance.

As discussed above, the final gray level is jointly determined by both panels. With simple calculations, all the possible gray levels are summarized in Table 1. Deleting the duplicated values, the total number of different gray levels is 17578 by combining two 8-bit LCD panels, which is larger than 14-bit signal depth modulation ( $2^{14} = 16384$ ). As mentioned above, the required operation voltage for a single-panel LCD with 14-bit grayscale is 131 V. Here, our cascaded LCD panels only requires  $V_{on} \sim 5$  V to get 14-bit signal depth. The power consumption and design complexity are dramatically reduced.

Table 1. Possible gray levels for two cascaded 8-bit LCD panels.

TN \ FFS	0	1	2	3	...	253	254	255
0	0	0	0	0	...	0	0	0
1	0	1	2	3	...	253	254	255
2	0	2	4	6	...	506	508	510
3	0	3	6	9	...	759	762	765
...	...	...	...	...	...	...	...	...
253	0	253	506	759	...	64009	64262	64768
254	0	254	508	762	...	64262	64516	64770
255	0	255	510	765	...	64768	64770	65025

### 3.5 Viewing angle

Figure 5(a) shows the simulated isocontrast contours for a conventional TN LCD. The highest CR is about 1200:1, and it drops gradually as the viewing cone increases. For some azimuthal angle, say  $230^\circ$ , it is less than 10:1, which means the image quality is degraded greatly. For FFS LCD [Fig. 5(b)], its CR could reach  $\sim 2500:1$ , but still drop to 100:1 at large viewing angles.

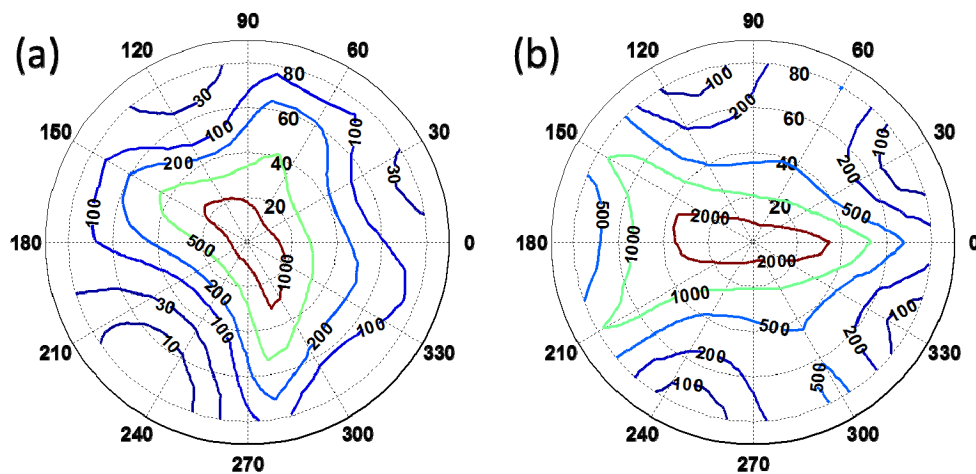


Fig. 5. Calculated isocontrast contour for (a) single TN panel and (b) single FFS panel.

When we cascade them together, the CR exceeds 1,000,000:1 within the  $\sim 20^\circ$  viewing cone, as shown in Fig. 6. Even for the entire viewing zone, CR still keeps over 1000:1. If we define the HDR requirement as 100,000:1, then the viewing angle in the horizontal direction is extended to about  $60^\circ$ . Meanwhile, since we use FFS as master display panel, its color shift

and gamma shift are very weak. If we combine with quantum dot backlight, then the color gamut of ~90% Rec.2020 can be obtained [23–25].

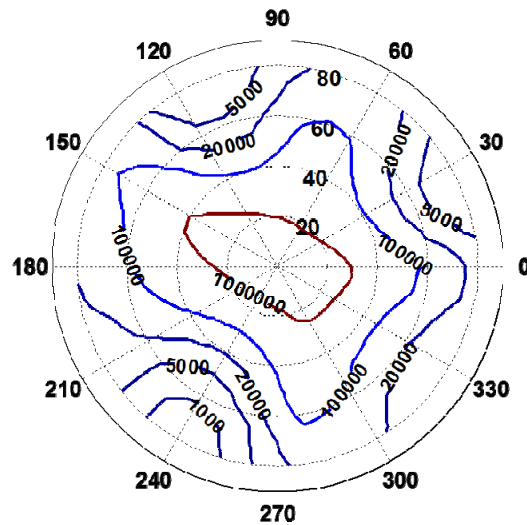


Fig. 6. Simulated isocontrast contour for the cascaded FFS and TN panels.

#### 4. Potential concerns

As above mentioned, dual LCD panels show great advantages in contrast ratio, signal depth and viewing angle. However, some challenges remain to be solved. The first one is increased cost, because two panels are used. Fortunately, the portion of panel cost to the total price is not high. For example, in a 5" FHD smartphone, the LCD panel is only \$15. Compared to the total price \$500 of a smartphone, the display part only occupies ~3%. For large size TVs, this portion increases, but is still acceptable. On the other hand, cost is less a concern for some high-end devices, like medical diagnosis, movie directing, photographers, universe detecting, art designers, etc.

Increased thickness is another potential concern for the dual LCD panels. For a conventional edge-lit LCD, the panel thickness is about 1.6 mm. And for direct-lit backlight with local dimming, the total thickness is ~5 mm. As shown in Fig. 1, in our design, one more LC panel is added, consisting of two polarizers ( $130\ \mu\text{m} \times 2$ ), two substrates ( $200\ \mu\text{m} \times 2$ ), LC layer ( $4\ \mu\text{m}$ ), and compensation films ( $150\ \mu\text{m}$ ). The increased thickness is ~0.9 mm. Therefore, for the whole device it is 2.5-mm thick, which is still ~2x thinner than the direct-lit display.

The other issue for dual LCD panels is decreased efficiency, which mainly results from the additional polarizers. Because of the absorption of polarizer, in our experiment, the optical efficiency of dual-panel system (i.e. FFS + TN) is reduced by 25% (surface reflection is considered), as compared to that of a single panel (i.e. FFS). Also, the electrical power consumption will also increase as two panels need to be driven independently.

Next issue is misalignment. If two LC panels don't align precisely, then the image would be distorted. Fortunately, this issue could be mitigated from image processing part. Guarnieri et al. developed a novel splitting algorithm to minimize the errors caused by misalignment [26, 27]. Based on their analysis, the images could still remain in good quality even though there is 3-pixel spatial shift between two LCD panels.

#### 5. Moiré effect

When two LCD panels are laminated together, Moiré effect appears because of the patterned TFT backplanes. To reduce this effect, a strong diffuser is often employed. But if we use such



a diffuser, the output light from the dimming panel will be depolarized and the overall performance degraded significantly. To overcome this problem, here we propose to use a new polarization dependent scattering film (PDSF) [28, 29], as depicted in Fig. 7. The system configuration is quite similar to that shown in Fig. 1; the only difference is that the analyzer in the dimming panel is replaced by a PDSF. This PDSF exhibits a unique property: polarization dependent scattering. For example, PDSF would scatter the s-wave strongly, while transmitting the p-wave. With this unique scattering property, Moiré effect is mitigated while keeping a high CR for the dual LCD panels.

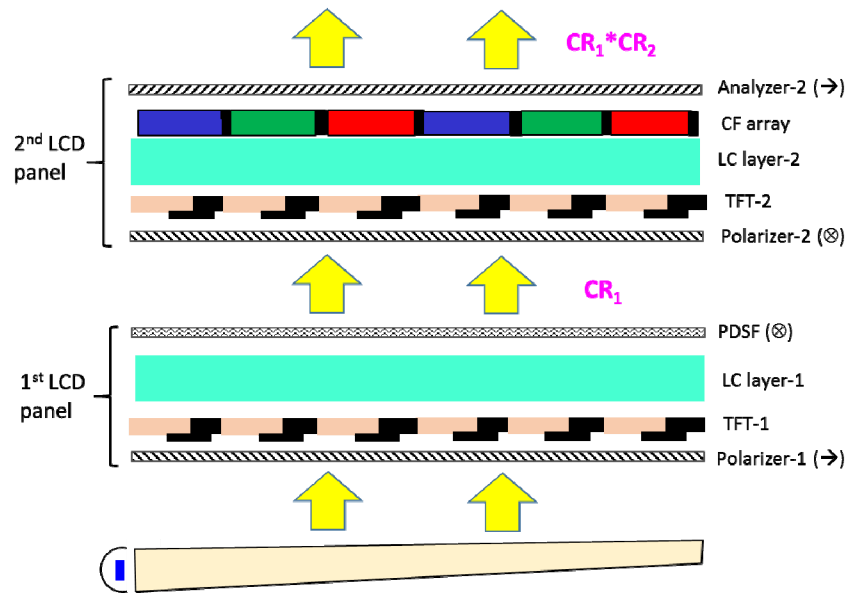


Fig. 7. Schematic diagram for the proposed structure using a PDSF to replace Analyzer-1.

To fabricate PDSF, in experiment we prepared a LC/monomer mixture consisting of BL038 (95.6 wt%), RM257 (4.2 wt%) and Irg651 (0.2 wt%). A homogeneous cell with cell gap  $d = 12 \mu\text{m}$  was employed. The LC test cell was first cured using a UV lamp ( $\lambda \approx 365 \text{ nm}$  and intensity  $5 \text{ mW/cm}^2$ ) for 30 s. After that we applied 20 V to the cell and cured it again for 1 hour with the same UV intensity. Then a multi-domain structure is obtained, as shown in Fig. 8(a). When the incident light is linearly polarized along x-axis [Fig. 8(b)], it gets scattered due to the non-uniform refractive indices in PDSF. Whereas for y-polarized incident light [Fig. 8(c)], the corresponding refractive index is uniform, i.e.  $n_o$ , therefore, it could traverse through PDSF without scattering.

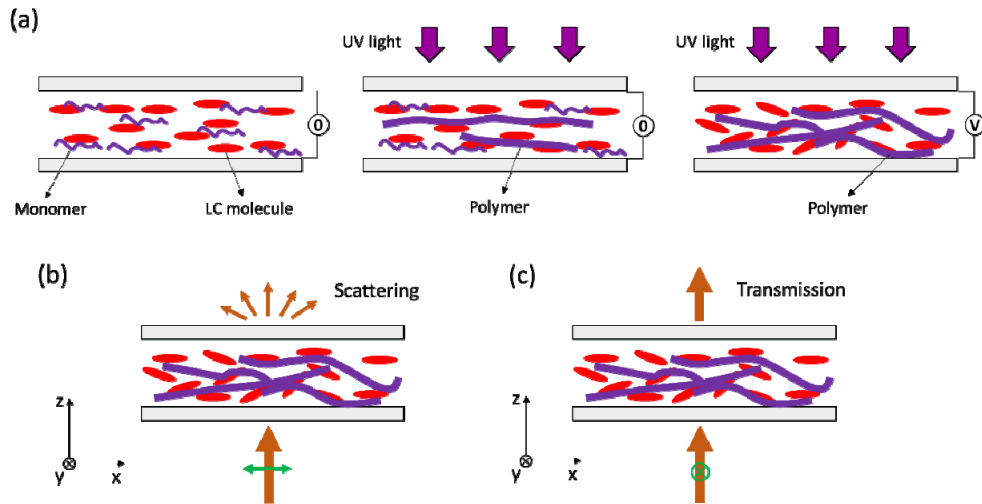


Fig. 8. (a) Schematic diagrams for the PDSF fabrications. Step 1: homogeneous state before polymerization; Step 2: polymerization without applied voltage; Step 3: polymerization with applied voltage. (b) Scattering state for x-polarized incident light. (c) Transmission state for y-polarized incident light.

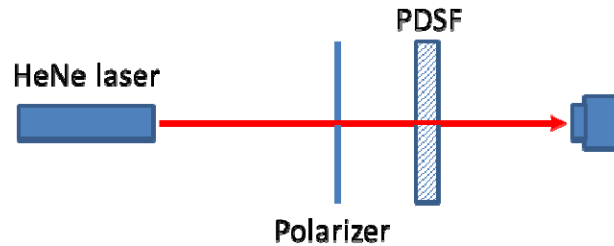


Fig. 9. Experimental setup for characterizing PDSF.

The measurement setup is depicted in Fig. 9, where a He-Ne laser was used as probing beam and the acceptance angle of the photodiode detector was  $4.5^\circ$ . When we rotate the PDSF, the incident polarization changes, as a result, the transmitted light intensity after PDSF changes accordingly. Figure 10 depicts the measured result. The peak transmittance for the p-wave is 75%, while in the scattering state (s-wave) the transmittance drops to 2.6%. The measured CR is about 28.6:1.

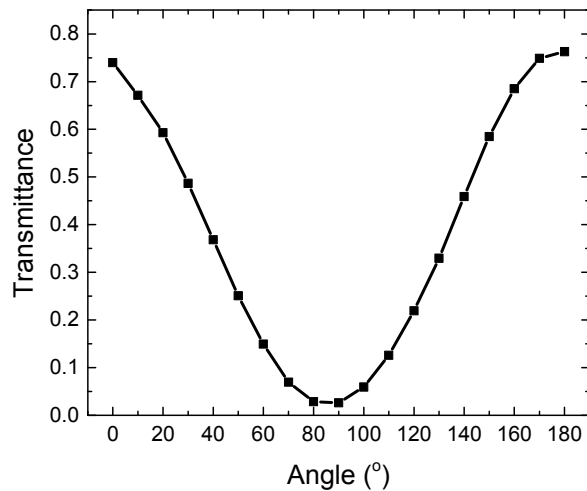


Fig. 10. Measured transmittance of PDSF at different polarization angles.  $\lambda = 633\text{nm}$ .

In another experiment, we measured the transmittance and scattering spectra of PDSF with a linearly polarized white light. Results are plotted in Fig. 11. As the wavelength decreases, the scattering gets stronger, leading to a decreased transmittance. Please note that even at clear state, the transmittance is still much lower than 100%. That means there is ~25% of the incident backlight is scattered. Such a light diffuser helps to suppress the Moiré effect, although the total optical efficiency is reduced. For practical applications, the transmittance and scattering properties of PDSF need to be optimized in order to eliminate the Moiré effect.

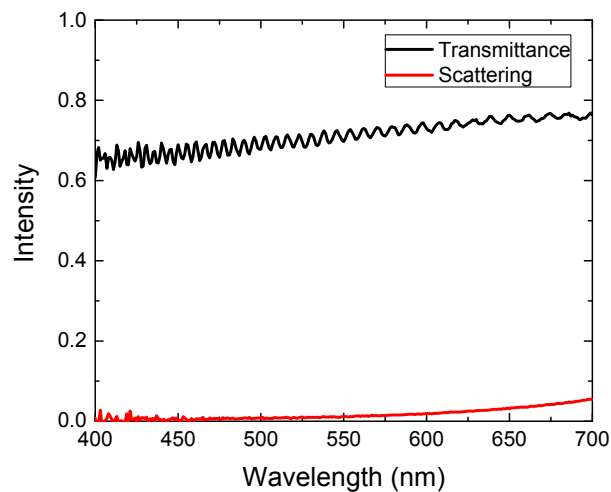


Fig. 11. Measured transmission and scattering spectra of the PDSF.

Next, we incorporate this PDSF with a TN cell to constitute the first LCD panel, and the obtained VT curve is plotted in Fig. 12. Clearly, the outgoing light intensity (backlight entering the master LCD panel) can be controlled pixel-by-pixel through the TN LCD. The required voltage is  $\leq 3\text{V}$ . When incorporating with our FFS cell, the measured CR is  $\sim 116,000:1$ , which is slightly higher than the desired value ( $> 100,000:1$ ) for HDR displays. To further improve the overall CR, PDSF should be further optimized, including its recipe, curing condition, and film thickness. Another option to boost the CR is to add the displaced Analyzer-1 back to the first LCD panel. That is, the PDSF film is positioned between Analyzer-1 and Polarizer-2, as Fig. 1 depicts. Under such a condition, an exceedingly high

CR can be restored, but the tradeoffs are increased panel thickness and ~15% lower light efficiency.

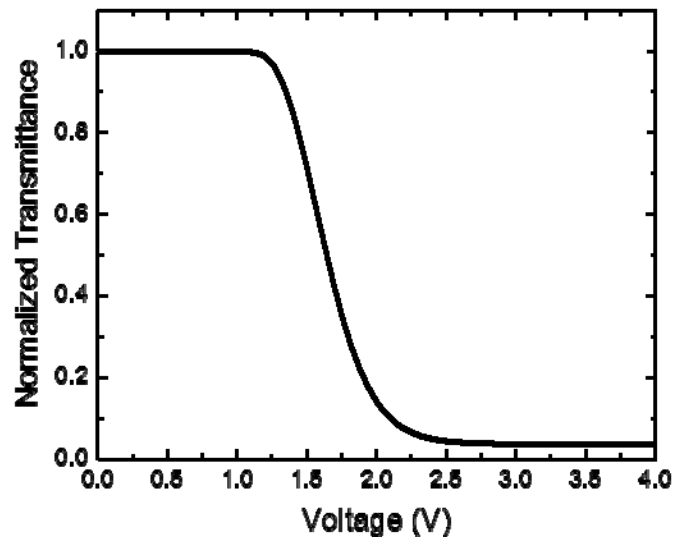


Fig. 12. Measured VT curve for PDSF with a TN cell.

## 6. Conclusion

We proposed a HDR display with two cascaded LCD panels and proved the design concept by using a FFS and a TN LC cells. The device performance is quite promising, including high contrast ratio ( $> 1,000,000:1$ ), high bit depth ( $> 14$  bits), and pixel-level local dimming. But some technical challenges remain to be addressed, such as pixel misalignment, decreased optical efficiency, increased panel thickness and power consumption. Also, Morié effect is a big problem, which degrades the image quality. To mitigate that, we added a polarization dependent scattering film between two LCD panels. Such a HDR display would find new applications for medical imaging, movies, and vehicular displays.

## Funding

AFOSR (FA9550-14-1-0279)

## Acknowledgments

The authors would like to thank Fenglin Peng and Guanjun Tan for helpful discussion, and a.u.Vista, Inc. for partial financial support.